

## STRUCTURAL DEFORMATION MEASUREMENT USING TERRESTRIAL LASER SCANNERS

**Stuart Gordon, Derek Lichti, Mike Stewart and Jochen Franke**

*Western Australian Centre for Geodesy  
Department of Spatial Sciences, Curtin University of Technology  
GPO Box U1987, PERTH WA 6845 Australia*

### Abstract

Deformation monitoring is typically undertaken with point-wise surveying techniques, such as total station or GPS. Terrestrial laser scanners (TLS) offer an opportunity to collect dense 3D point data over an object or surface of interest. The single point precision of medium to long-range TLSs varies from  $\pm 2\text{mm}$  to  $\pm 25\text{mm}$ , depending on the instrument model and observation conditions. However, the theoretical precision of a surface derived from spatially dense point cloud data is substantially higher than the single point precision. This paper presents results from two experiments designed to explore the achievable precision of TLSs for surface deformation measurement. In each experiment, it was shown that the TLS systems were able to measure vertical deflection at six to 12 times better than their advertised single point precision. In one test, a TLS (single point precision of  $\pm 6\text{mm}$ ) achieved an accuracy of  $\pm 0.5\text{mm}$  (RMS).

### 1. Introduction

Terrestrial laser scanners (TLSs) offer an opportunity to collect dense 3D point data over an entire object or surface of interest. The dense dataset can be modelled to generate a best-fitting surface. The precision of a modelled surface derived from spatially dense point cloud data is substantially better than the single point precision of the raw data.

The single point precision of medium- to long-range TLSs is relatively coarse and varies from  $\pm 2\text{mm}$  to  $\pm 25\text{mm}$ , depending on the instrument model and observation procedures. However, techniques may be employed to improve the single point precision of a TLS system. One method involves averaging repeat scan clouds. Multiple scans acquired sequentially are averaged to create a cloud that may be two to three times more precise than an individual cloud, according to the root of the number of repeat scans. For example, four repeat scans will theoretically improve the standard deviation of a single point by a factor of two (*e.g.* Amann *et al.*, 2001). This has been empirically verified by Lichti *et al.* (2002b).

A logical application of TLS is in the field of deformation monitoring. TLS offers advantages such as remote measurement, a permanent visual record and high spatial data density, as does photogrammetry, although, without the requirement of targets (for non-episodic monitoring). It yields observations in all three dimensions unlike common contact sensors that are usually employed in deformation monitoring. However, the perceived poor precision of TLS systems has precluded their use in the past (*e.g.* Fraser and Riedel, 2000).

This paper presents an investigation designed to explore the sensitivity of TLS systems for structural deformation monitoring tasks. Two experiments were performed involving controlled load testing of structures. Induced deformation was at the millimetre level and up to several centimetres. Close-range photogrammetry and contact sensors were used to benchmark test the laser scanner data.

## 2. Instrumentation

Two TLSs were used during these tests. A Cyrax 2500 (Cyra, 2002) is a high accuracy, high resolution scanner. It has a quoted single point accuracy of  $\pm 0.006\text{m}$  ( $1\sigma$ ) at a data capture rate of 1000 points per second. The field of view (FOV) of this fixed-head instrument is  $40^\circ$  by  $40^\circ$ . The second scanning system used during testing was an I-SiTE R-350 (I-SiTE, 2002). At the core of this scanning system is a Riegl LMS-Z210 (RIEGL, 2002) laser scanner. The LMS-Z210 has a single point accuracy of  $\pm 0.025\text{m}$  ( $1\sigma$ ) and a data capture rate of 6000 points per second. The angular FOV of the LMS-Z210 is  $80^\circ$  in the vertical direction ( $40^\circ$  above and below the horizontal plane) and  $340^\circ$  in the horizontal direction. A comprehensive overview of TLS operation may be found in Lichti *et. al.* (2002a).

Close-range photogrammetry was used to control both experiments. A Kodak DC420 with a CCD array of 1524 by 1012 pixels (square pixels with a  $9\mu\text{m}$  width) was fitted with a 14mm lens. The focal ring was set to infinity and secured with tape. The camera was calibrated before and after each experiment and each calibration compared for consistency (*i.e.* statistical testing of the focal length for change between photogrammetric campaigns).

Dial gauges and linear variable-differential-transformers (LVDTs) were also employed as an independent benchmarking measurement source. They are both capable of measuring in a single dimension. Depending on the setup and requirement, this is typically in either a vertical or horizontal axis. The resolution of a dial gauge is at the 0.01mm level. LVDTs can be sensitive to deformation as small as  $0.5\mu\text{m}$  (Dyer, 2001). Due to their contact nature, dial gauges and LVDTs must be removed from a structure if destructive testing is planned, unless they are to be sacrificed. More information about LVDTs can be sought from sources such as Doebelin (1990) or Dyer (2001).

## 3. Experiment I: Wooden Beam

The first experiment involved the controlled loading of a wooden beam in an indoor test frame based in the Department of Civil Engineering laboratories at Curtin University. The beam, which had dimensions of 5.2m x 0.2m x 0.1m, was supported at each of its ends. The loading was applied by a hydraulic jack which was positioned at the centre of the beam. Fig. 1 shows the beam *in situ* prior to the testing and the position of the jack.



Fig. 1: Wooden beam, hydraulic jack system, reflective targets and the Cyrax 2500.

A total of eight load increments were applied whereby a nominal 5mm of vertical displacement (at the centre of the beam) was induced on each occasion. A “dead load” was collected at the beginning of the testing allowing the capture of a zero-load case. A dial gauge was positioned in the approximate centre of the beam and was used by the jack operator to assist in determining each 5mm increment (it was not used for analysis). The total downward vertical deflection was approximately 40mm.

### 3.1 Data Collection

The Cyrax 2500 was located 5.4m from the centre of the beam and to the left of the laboratory (see Fig. 1) and an I-SiTE R-350 was positioned 6.4m from the centre of the beam away to the right of the laboratory. Both instruments were set up on stable footings and were not moved for the entire experiment. It was assumed that the TLSs were undisturbed for the duration of the testing. Neither instrument was force-centred over a pre-marked known point. The I-SiTE R-350 was levelled but the Cyrax 2500 was not (it does not have a level bubble).

The Cyrax 2500 initially captured a high resolution scan of the entire vicinity of the beam (including testing frame and the wall behind the frame) ensuring that all photogrammetric targets were included. This was specifically undertaken to enable identification of targets allowing the resection of the scanner. In subsequent scans using the Cyrax 2500, the FOV was programmed to exclusively capture the beam thus reducing the scan time. During testing, high-resolution scans were collected at each epoch by each of the scanners. The Cyrax 2500, which has a relatively slower data capture rate than the I-SiTE R-350, only acquired a single scan per load epoch. The I-SiTE R-350, which offers a relatively coarser single point accuracy than the Cyrax 2500, captured three repeat scans of the beam that were averaged to produce a single mean scan, theoretically reducing the standard deviation of individual points to  $\pm 14\text{mm}$ .

Close-range photogrammetry was used to control the experiment using 25 targets on the face of the beam (see Fig. 1). Many other targets were placed around the room and on stable components of the test frame. The photogrammetric coordination of the array of targets also provided a common coordinate system for the TLS datasets.

Three dial gauges were situated under the beam on a stable foundation and arranged so that they were able to measure vertical displacements. The measurements were recorded during the experiment by reading the dial of each gauge.

### 3.2 Photogrammetric Results

The first task was adjusting the photogrammetric data. This was performed using *Australis* (Fraser and Edmundson, 2000) digital photogrammetric software. The photogrammetric network was treated as a free network adjustment and the datum was defined by the stable targets. The RMS of coordinate standard deviations of the stable targets was  $\pm 0.14\text{mm}$  ( $1\sigma$ ) and  $\pm 0.15\text{mm}$  ( $1\sigma$ ) for X and Y, respectively and  $\pm 0.04\text{mm}$  ( $1\sigma$ ) for Z – the most crucial direction for this experiment.

Comparison of the dial gauge measurements with the photogrammetric measurements was performed. The largest difference was 0.22mm, which was between the ‘left’ dial gauge and its corresponding located target at the 25mm deflection case. There was a booking error for the ‘right’ dial gauge during the 35mm deflection case, therefore, it was omitted from the analysis. The differences between photogrammetry and the dial gauges may, in part, be blamed on misalignment of the targets with the dial gauges. The overall RMS of differences between the photogrammetric vertical deflections and the dial gauge measurements was  $\pm 0.11\text{mm}$ , which was consistent with the expected photogrammetric precision.

### 3.3 TLS Results

Processing of the laser scanner data involved four main steps: (i) resection and transformation into the photogrammetric reference frame; (ii) manual extraction of the beam from each scan cloud; (iii) gridding the top surface of the beam; and (iv) interpolating the height of the photogrammetric targets. Since both TLSs were set up at different positions, both scanners used the targets coordinated by the photogrammetric process to resect their position and orientation. The dead load case for each TLS was used for this purpose. Once the resection parameters were

derived, subsequent clouds were transformed. A total of 11 control points were used for the Cyrax 2500 resection and 15 control points were used for the I-SiTE R-350 resection. Whilst the transformation process will serve as an additional error source (Gordon and Lichti, 2003), it was a necessary task to enable direct comparisons of vertical deflections from the photogrammetric and TLS data sources.

Once all scan data were in the same reference frame, the individual scan clouds were manually edited to remove all scan points except for the those on the top of the beam. The top of the beam was used for analysis because it best represented the vertical deflection – the most pertinent for subsequent structural analyses. The extracted beam top clouds, though composed of irregularly spaced points, had an approximate sample interval of 5mm for the Cyrax 2500 and 15mm for the I-SiTE R-350. Gridding was employed to obtain a continuous surface represented by a regularly spaced grid of points. The dead load epoch from each TLS was used to define the spatial extents for the gridding process. Each scan cloud was gridded using triangle-based cubic interpolation with a grid spacing of 5mm for the Cyrax 2500 data and 10mm for the I-SiTE R-350 data.

Analysis was undertaken by comparing the deflection of the photogrammetric targets with the deflection of the gridded surface at a point near each target. Each photogrammetric target was projected along a horizontal plane into the spatial extents of the gridded surface. The height of the projected target was then interpolated with bicubic interpolation using the TLS gridded surface and its planimetric position.

The direction of the projection was calculated by finding the 2D line of best fit (in the X-Y plane) of the photogrammetric targets. Once the equation of the line was determined, the line orthogonal to that was used (at each target location) to project the photogrammetric targets into the surface of the beam (see Fig. 2). This ensured that each target would be projected into the surface at a normal angle to the wooden beam. A projection distance of 75mm for the Cyrax data and 100mm for I-SiTE was used. These distances were arbitrarily chosen large enough to avoid any possible edge effects brought about by the gridding. A total of 13 photogrammetric targets, constituting the entire top row, were interpolated in this way and were available for analysis for each load epoch.

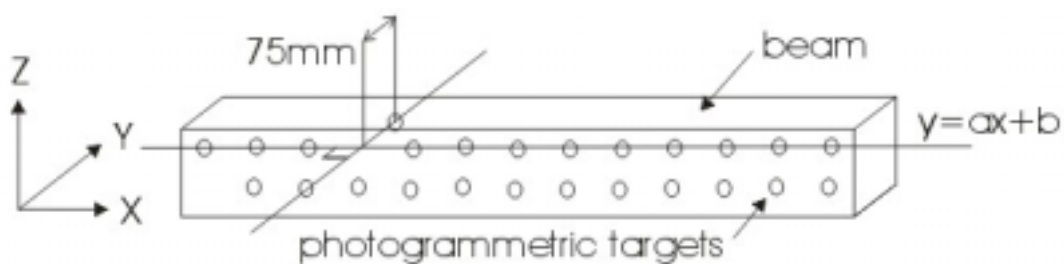


Fig. 2: Projecting photogrammetric targets onto gridded surface.

Table 1 shows the results for this method. The values are RMS of differences, which were generated by comparing the height coordinate of a target (determined by the photogrammetric process) with the interpolated height of the same target (based on the gridded TLS data). This was done for all 13 targets in each of the eight deflection cases.

<b>Vertical Deflection</b>	<b>Cyrax 2500</b>	<b>I-SiTE R-350</b>
5mm	±0.57mm	±4.6mm
10mm	±0.42mm	±4.3mm
15mm	±0.56mm	±5.1mm
20mm	±0.66mm	±4.8mm
25mm	±0.41mm	±3.5mm
30mm	±0.42mm	±4.1mm
35mm	±0.62mm	±4.4mm
40mm	±0.49mm	±4.5mm
<b>Total RMS</b>	<b>±0.52mm</b>	<b>±4.4mm</b>

Table 1: Comparison of TLS Deflections and Photogrammetrically Derived Deflections.

All differences yielded by the gridded Cyrax 2500 data were less than one millimetre. The total RMS for the Cyrax was  $\pm 0.52\text{mm}$ , which is eleven times better than its single point accuracy. The largest RMS difference was  $\pm 0.66\text{mm}$ . The total RMS of differences of the I-SiTE R-350 was  $\pm 4.4\text{mm}$ , which is nearly six times better than its single point precision. However, these data were constructed using three repeat scans, therefore, the theoretical single point precision is  $\pm 14\text{mm}$ . In this case, the RMS of differences is only three times better than this single point precision. Whilst this is a very good result, better results may have been achieved with the I-SiTE if the point density of the I-SiTE was higher. There were many sparse areas on the beam top with all I-SiTE acquired scan clouds. Selecting a smaller sampling interval would have increased the number of points on the beam, however, time constraints precluded this from being undertaken. The instrument set up suffered from the laser beam striking the wooden beam top at a grazing angle potentially causing imaging errors, such as shape distortion (Lichti *et al.*, 2002b). Setting the instrument at a higher elevation may have improved the definition of the beam top.

#### 4. Experiment II: Concrete Beam

A second experiment was conducted whereby an “L-shaped” (in cross section)  $7.2\text{m} \times 0.5\text{m} \times 0.5\text{m}$  reinforced concrete beam was loaded until failure. The beam was formerly part of an old bridge, which had been dismantled for the purpose of controlled laboratory testing. The beam was placed in an outdoor testing frame and supported at each end. The two load points were near the centre of the beam. The purpose of this experiment, from a measurement context, was to recover increments of vertical deformation (corresponding to each load epoch) up to an anticipated  $40\text{mm}$ .

##### 4.1 Set Up and Targeting

An I-SiTE R-350 was situated  $7\text{m}$  from the beam and directly in front of the test frame (see Fig. 3). It was set up as high as possible on the tripod enabling acquisition of scan points from the top surface of the beam. The scanner was not levelled or setup over a known point. Similar to the first experiment, the position and orientation of the TLS was determined by resection. The photogrammetric coordinate system provided the reference frame for the experiment. Fig. 3 shows the reflective targets on the beam, test frame and stable white wall (at rear left). The targets were retroreflective circles adhered to a square matte black card background. The diameter of the targets varied from  $16\text{mm}$  to  $25\text{mm}$  according to their distance from the camera (and the scale of the photography). A large concrete block and long black metal beam were placed behind the concrete specimen (at rear right) as an additional surface for targeting thus further densifying the array of stable targets.



Fig. 3: Concrete beam (in the load testing frame) and the I-SiTE R-350 instrument.

#### 4.2 Data Collection

A total of 13 measurement epochs were acquired during the period of testing where the equivalent of 49t (applied by two hydraulic jacks) was required to cause the specimen to fail. A dead load epoch was acquired at epoch 0 and also at epoch 7 (where the load on the beam was relaxed). The final measurement epoch where the beam was intact was epoch 12, however, contact sensors were removed prior to this (after recording epoch 11) because failure was imminent. At each epoch, a total of three repeat scans were collected and averaged to produce a single mean scan.

Each photogrammetric epoch consisted of nine images from around the front of the beam ensuring strong convergent imaging angles. Some of the exposures were taken at ground level whilst others were captured when standing on a 2m high stockpile of wooden beams and other wooden members (from a dismantled bridge) at the rear of the instrument. This enabled photographs to be collected with good convergent angles in height as well as in the horizontal.

Fig. 4 shows the front of the beam, the two jacks and a number of the contact sensors *in situ* in front and behind the beam. Two LVDTs were placed at the front of the beam and aligned to measure vertical displacement. Two dial gauges were used to measure horizontal displacement and were co-located with the LVDTs. However, they were not used in this investigation. At each of these locations, photogrammetric targets were adhered to the beam.



Fig. 4: Photogrammetric targets co-located with dial gauges and LVDTs.

#### 4.3 Results

Photogrammetric adjustment was undertaken in a similar fashion to the first experiment. The RMS of the estimated coordinate precision of the photogrammetric targets was  $\pm 0.12\text{mm}$  ( $1\sigma$ ),  $\pm 0.21\text{mm}$  ( $1\sigma$ ) and  $\pm 0.09\text{mm}$  ( $1\sigma$ ) for X, Y and Z respectively.

Resection was performed for the TLS using the dead load cloud (epoch 0) and 12 control points coordinated by the photogrammetry. The position and orientation parameters were used to transform each of the remaining scan clouds. Once georeferenced, the top of the concrete beam (lower section of the two top surfaces) was manually extracted from each scan cloud.

The scan data of the tops of each beam were gridded in a similar fashion to the previous experiment. Table 2 shows the results for the triangle-based cubic grid interpolation method with a grid spacing of 10mm. The method of target projection was again utilised, using a projection distance of 75mm and bilinear interpolation to compute the height of the projected target. Approximately 10 to 14 targets were available for the comparison of each epoch. The number of targets depended on their visibility during the capture of photogrammetric imagery.

<b>Epoch</b>	<b>1</b>	<b>2</b>	<b>3</b>	<b>4</b>	<b>5</b>	<b>6</b>	<b>7</b>	<b>8</b>	<b>9</b>	<b>10</b>	<b>11</b>	<b>12</b>	
<b>Load (kN)</b>	40	80	120	160	200	240	0	80	160	240	360	450	
<b>Vertical Deflection (mm)</b>	2.1	4.1	6.0	8.0	10.0	12.9	0.9	4.1	8.3	13.2	28.8	48.3	<b>Total RMS</b>
<b>RMS (mm)</b>	1.5	0.8	2.1	1.1	1.7	2.1	1.1	2.4	1.8	2.3	2.8	3.1	<b>2.0</b>

Table 2: RMS of differences for different interpolation methods and grid spacing.

The scanner-derived vertical deflections compared to the photogrammetry have an RMS of differences of  $\pm 2.0$ mm. This is over an order of magnitude better than the single point precision of the I-SiTE R-350 ( $\pm 25$ mm). It is seven times better than the instrument's theoretical single point precision after averaging three repeat scan clouds. It is noted that, similar to the wooden beam test, the concrete beam top was scarcely populated with laser scan points. It is not known why this result is better than the wooden beam test. Despite similar experiment design, the imaging geometry of the concrete beam test may be considered more favourable due to the higher elevation of the instrument relative to the top surface of the beam.

## 5. Conclusions and Recommendations

Two experiments have been presented where TLSs have been used for structural deformation tests. It has been shown that with simple processing strategies, normally coarse accuracy TLS instruments can be used to measure small deformations (less than 3mm in some circumstances) with high precision. The I-SiTE R-350 ( $\pm 25$ mm) recovered vertical deformation, with respect to the benchmark photogrammetric data, with an RMS of  $\pm 2.0$ mm for the concrete beam test and  $\pm 4.4$ mm for the wooden beam test. It is not known why there is a disparity of results for the same instrument but a poorer imaging geometry (at the wooden beam test) is the most likely reason. The Cyrax 2500 ( $\pm 6$ mm) proved more reliable and exhibited an RMS of differences of  $\pm 0.5$ mm for the wooden bearer test. It was expected that the Cyrax 2500 would perform better than the I-SiTE R-350 because it is a more precise instrument offering a higher sampling resolution using a much smaller spot size.

The physical set up of the TLS is an important consideration. Ideally, the laser scanner should be positioned to maximise capture of the surface that would best represent the deformation. In these experiments, this was the top surface of the specimen. The wooden bearer test demonstrates that poorer results will occur if this condition is not properly observed. Despite this necessity, the concrete beam experiment showed that it was still possible to successfully measure deformation even though the imaging geometry was suboptimal and scan data were scarce.

Selection of the most appropriate surface modelling technique is of critical importance and is an on-going focus of investigation. Gridding was used exclusively in these experiments and the selection of interpolation method employed is also part of continuing research, as is selection of optimal grid spacing. The latter is dependent on the original sampling interval of the TLS. The

choice of surface modelling technique is a function of the complexity of the shape. Both beams (concrete and wooden) had inherently flat top surfaces which were relatively simple to model. Further research is also encompassing the use of 'virtual features' for assisting deformation measurement. That is, the intersection of two surfaces (*e.g.* planes) producing a three dimensional line or edge is a feature that can be replicated and used for monitoring purposes.

These tests were designed for close-range measurement over a monitoring period of a couple of hours. Further research will expand to include testing over longer ranges and monitoring of surfaces over a prolonged time schedule (*e.g.* weeks or months). In this case, the instrument will require spatial referencing to previous measurement epochs thus presenting an additional error source. Furthermore, future work will include resolving deformation in all three dimensions.

## Acknowledgments

The authors wish to thank Gerry Nolan and Dale Keighley from McMullen Nolan and Partners Surveyors (Perth, WA) for the use of their Cyrax 2500 system. Testing of the beams were conducted under the supervision of Dr Ian Chandler, David Chandler and staff from the Department of Civil Engineering, Curtin University for which the authors are grateful.

## Bibliography

- Amann, M. C., T. Bosch, M. Lescure, R. Myllyla and M. Rioux (2001). Laser Ranging: A Critical Review of Usual Techniques for Distance Measurement. *Optical Engineering*, 40(1), 10-19.
- Cyra (2002). *Cyra Homepage*, <http://www.cyra.com>.
- Doebelin, E. O. (1990). *Measurement Systems: Application and Design* (4th Ed.), McGraw-Hill Publishing Company, Singapore, 960 pp.
- Dyer, S. A., (Ed.) (2001). *Survey of Instrumentation and Measurement*. John Wiley and Sons, New York, USA, 1096p.
- Fraser, C. S. and K. L. Edmundson (2000). Design and Implementation of a Computational Processing System for Off-Line Digital Close-Range Photogrammetry. *ISPRS Journal of Photogrammetry and Remote Sensing*, 55(2), 94 - 104.
- Fraser, C. S. and B. Riedel (2000). Monitoring the Thermal Deformation of Steel Beams via Vision Metrology. *ISPRS Journal of Photogrammetry and Remote Sensing*, 55(4), 268-276.
- Gordon, S. J. and D. D. Lichti (2003). Terrestrial Laser Scanners with a Narrow Field of View: The Effect on 3D Resection Solutions. *Survey Review*, In Press.
- I-SiTE (2002). *I-SiTE Homepage*, <http://www.isite3d.com>.
- Lichti, D. D., S. J. Gordon and M. P. Stewart (2002a). Ground-Based Laser Scanners: Operations, Systems and Applications. *Geomatica*, 56(1), 21 - 33.
- Lichti, D. D., S. J. Gordon, M. P. Stewart, J. Franke and M. Tsakiri (2002b). Comparison of Digital Photogrammetry and Laser Scanning. *Proceedings of CIPA WG 6 International Workshop on Scanning Cultural Heritage Recording*, Corfu, Greece, 1 - 2 September, 39-44.
- RIEGL (2002). *RIEGL Laser Measurement Systems*, <http://www.riegl.com>.